Title: Looking inside an avalanche using a novel radar system

Authors: C.J. Keylock[1], M. Ash[2], N. Vriend[3], P. V. Brennan[2], J. N. McEwaine[4], B. Sovilla[5]

[1] Department of Civil and Structural Engineering, University of Sheffield, Mappin Street, Sheffield, S1 3JD, c.keylock@sheffield.ac.uk

[2] Department Electronic and Electrical Engineering, Gower Street, University College London, London, UK.

[3] Department of Applied Mathematics and Theoretical Physics, University of Cambridge, Cambridge, UK.

[4] Department of Earth Sciences, University of Durham, Durham, UK.

[5] WSL Swiss Federal Institute for Snow and Avalanche Research, SLF, Davos, Switzerland.

Abstract

Introduction

Debris flows, pyroclastic flows, lahars, and rock and snow avalanches are all rapidly moving mass flows that are released from steep slopes and have caused tens of thousands of deaths in the last century. In the case of debris flows and lahars, the debris is mobilised with very significant water content and while the upper surface of the flow interacts with the surrounding air, the primary aim of current scientific work is to understand how the varying proportions of debris and water, and the nature of the underlying substrate affect the flow dynamics. Richard Iverson recently provided an up-to-date review of this field in *Geology Today*.

While slush and wet snow avalanches also contain significant free water content, attention generally is focussed on the dry events, where the dynamics concerns snow and air. As

Figure 1 shows, this gives a snow avalanche a strong visual resemblance to a pyroclastic flow, where the entrainment of air into the head of the flow results in a highly turbulent outer layer (the powder cloud) with a volume fraction of snow that is only about one percent and a density that varies as more and more ambient air is entrained. For both pyroclastic flows and avalanches, there is a much denser layer flowing undercover of this suspended gravity current. Because of the temperatures within a pyroclastic flow, risk zoning focuses on the outer layer as it tends to travel furthest and at greatest speed, while still being immensely destructive. In the case of avalanches, the suspended powder cloud typically travels further and perhaps 50 % faster. However, impact pressures are based on the product of density and velocity squared and this difference in speed is not sufficient to outweigh the more than ten-fold difference in density between the powder cloud and the dense, flowing layers. This form of analysis underplays the fact that the powder cloud, which may be 50 m or more high, will envelop a whole building, exerting a force over the full vertical extent, while the dense layer will be 1 m – 2 m thick.

For those towns and villages in alpine regions exposed to potential avalanching, both components of the flow can generally attain the valley floor. In all but the largest events the dense flow is the most destructive and the powder cloud does little damage. However, in the largest events the extremely high speed and size of the powder cloud can damage large structures.

This represents a fundamental problem for avalanche science because the dynamics of this component of the flow are deemed to be critical yet they cannot be clearly observed. Only

when the flow stops and the powder cloud settles out can the run-out deposit of the dense layer and the damage it has done be seen (Fig. 2). Consequently, while debris flow scientists can make use of optical techniques to visualise the dense layer dynamics, to understand the dynamics of snow avalanches (and by implication, pyroclastic flows), we need to move into a different part of the electromagnetic spectrum.

Existing methods for radar imaging of snow avalanches

At present, radar systems are used in two main ways in avalanche science. In the first case, they are buried in the avalanche path and look up into the flow. In this way, we can obtain information on erosion rates by the different components of the flow (Fig. 3). Our ability to do this demonstrates why studying avalanches presents a significant advantage over more conventional geological mass flows: in the summer we can go and check our instruments and the electronics housed underground; they are not buried beneath 5 metres of solid rock. These radar systems can also be installed close to other sensors in the path that are also likely to survive a flow, meaning that it is possible to relate information from various sensors to gain a greater understanding of the dynamics. For example, Figure 4a is taken from the Vallée de la Sionne test site in Switzerland. It shows the underground alcove in the avalanche path housing the electronics that records the data from the various sensors and relays it down to the bunker at the foot of the mountain. Figure 4b shows the main instrument pylon in the path, which contains optical sensors for estimating velocities at different heights, switches that log the maximum depth of the dense layer, and a pressure sensor high on the pylon for obtaining information on the powder cloud dynamics. Adjacent to this is a wedge where a load plate records the force exerted by the dense layer.

In the second application of radar, the instrument is placed at the bottom of the mountain and attempts to image the whole flow as it moves downslope. Until very recently, the best instrument for this work was developed by Helmut Schreiber at the University of Graz, and deployed at test sites in Norway and Switzerland. However, the range resolution for this instrument is not sufficient to provide a direct comparison with the velocities estimated with other sensors: Sensors on the pylon produce velocity estimates by cross-correlating measured properties to derive a time lag over a known (short) distance and, thus, point estimates of the velocity at sub-metre resolution, this radar averages over a 30 m distance. Hence, while it provides useful data for seeing if velocity estimates from numerical models are broadly correct, the data are not of a resolution to be coupled directly to the point estimates and to infer detail of the flow physics. Our research has enhanced the capability of this type of radar application.

Our new radar instrument

Our radar emits a continuous wave, but modulates the frequency of the signal that is output to give a series of six linear frequency ramps (also known as chirps) with 1, 2, and 5 millisecond durations. As shown in Fig. 5a, it takes 0.02 seconds to transmit this signal, meaning that we can obtain data from a given chirp fifty times a second. The gaps that can be seen between each up and down chirp also appear in the data returned from the avalanche as they mark a period of no modulation. Looking for these gaps makes it easier to assign the returned signal to particular transmitted chirps during post-processing of the

data. The signal is made up of six chirps of varying periods, each with their own merits. The measurements taken using the shorter period chirps (left-hand side of Fig. 5a) are distorted less by Doppler shifts caused by moving targets as they have coarser Doppler resolution (given by the inverse duration of the chirp). The longer period chirps (on the right-hand side of Fig. 5a) allow for measurements of the entire avalanche track as they provide a longer maximum unambiguous range. In practice, we have found the longest period chirps to be of greatest use as they provide good signal-to-noise ratio measurements all the way to the top of the mountain (just over 2500 m away). Indeed, their disadvantage of being more distorted by Doppler shifts can be resolved by combined processing of the up and down chirps as the Doppler affects their return signals in an equal and opposite way

The 200 MHz variation on each chirp provides a maximum range resolution of 0.75 m, which compares very favourably indeed with the 30 m of the older instrument described above. (The resolution is given by $c/2b$, where c is the speed of light and b is the sweep bandwidth). This range resolution is of a similar order of magnitude to the largest individual blocks in the avalanche and to the averaging distance used by the instruments on the pylon (Fig. 4b).

Our radar transmitter is mounted on the side of the bunker at Vallée de la Sionne (Fig. 5b). The signal shown in Fig. 5a is transmitted from here for the duration of the avalanche and the reflected signal is detected by the eight receivers also mounted on the bunker (Fig. 5b). In fact, we have two sets of receivers – one mounted inside the bunker for use during targeted artificial release experiments when the bunker is manned, and the other mounted

on the outside for use when avalanche activity in the path is detected automatically (obscured by the open shutters in Fig. 5b). So far, our data have been of the latter type. This use of eight receivers also extends the capability of our instrument over pre-existing technology, which was a simple range radar. Because the eight receivers detect a return at different times, by appropriate design of the separation between receivers, we can obtain azimuthal (cross-path) information, permitting us to separate out flow fronts travelling down different gullies, detect the instrument pylon in the path and, potentially, to track individual large blocks within the flow as long as they maintain a strong reflection. Compared to a range resolution of 0.75 m, our azimuthal resolution is rather less. The width of the receiver array is 7 m, which gives an angular resolution of around 0.6 degrees corresponding to just under 10 m resolution at 1 kilometre. The current array is also sparse so there are some ambiguities that will be removed in an upgrade where we will adopt a dense collection of receive antennas to improve the array response.

Results so far

A sketch of the Vallée de la Sionne avalanche path is shown in Fig. 6, showing the location of the bunker (Fig. 5b), the instrument pylon (Fig. 1, Fig. 4b) and the locations of the buried, upward looking radar pairs (data from which are shown in Fig. 3). During an artificial release, explosives are set off in one of the three starting zones (labelled *PR*, *CB1* and *CB2* in Fig. 6) and pre-release checks ensure that all sensors are operating, meaning that data from all instruments, including video footage can be compared. As already noted, our data so far have been from automatic releases that lack video footage. However, we have been able to obtain comparisons to velocity data recorded at the pylon and from the buried radar

(positions shown by *A*, *B*, and *C* in Fig. 6) and these have been very successful. Hence, we have some confidence that our instrument provides the first ever, high quality velocity dataset of a flow mass movement for the majority of the duration of the flow.

An example of our results are shown in Fig. 7. The data are obtained using the right-most chirp in Fig. 5a, with data averaged over all 8 receivers shown in Fig. 5b. From the slope of range versus time we can obtain accurate estimates of the main front of the flow, with very high velocities (~ 60 m s^{-1}) recorded until a range of 500 – 700 m, where the slope reduces, and the velocity drops to ~10 m s^{-1}. Multiple flow fronts exist in Fig. 7 and their crossing is an artefact of the nature of this plot. By averaging across all receivers we lose azimuthal resolution. In reality, these fronts are occurring in different gullies (Fig. 6c). Subsequent processing of the azimuthal information has revealed that Front 1 on Fig. 7 was made up of two separate fronts some 40 m wide and 70 m apart at upslope of range of 1220 m, which then merged at this distance (Fig. 7). In addition, behind the main fronts, Fig. 7 reveals separate surge fronts as well as finer scale instabilities.

Conclusion

These unprecedented data have the potential to yield significant insights into the physics of these flows. As yet we have primarily worked on the validation of the measurements, but we now have confidence to examine the detailed physics as well as the intrinsic variation of flows occurring on the same path as a function of snow conditions (e.g. wetter snow tends to flow at lower velocity), conditions in the path (lots of fresh snow in the path is likely to be eroded increasing the mass of the flow), and the size of the event. From these data, we will

be able to examine the weaknesses of existing models for the dynamics of these flows and propose enhancements. This will lead to more accurate risk zoning for avalanche studies and an improved ability to model the interaction of a flowing avalanche with a building, or a defensive wall, enhancing building regulation and the design of defence structures. The enhancements we have planned for the radar, in particular, the improved azimuthal resolution, will develop the capability of this technology further.

We also believe that these results will be of direct utility to those working in allied disciplines such as pyroclastic flow dynamics. Furthermore, we would hope in the future to move a similar instrument to this to a safe location and study such flows directly, meaning that risk zoning for pyroclastic flows can also be improved.

Suggestions for Further Reading

Ash, M., Brennan, P. V., Lok, L. B., McElwaine, J. N., Vriend, N. M., Keylock, C. J., Sovilla, B. 2014. Two-dimensional radar imaging of flowing avalanches, *Cold Regions Science and Technology*

Gauer, P., Issler, D., Lied, K., Kristensen, K., Iwe, H., Lied, E., Rammer, L., Schreiber, H. 2007. On full-scale avalanche measurements at the Ryggfonn test site, Norway, *Cold Regions Science and Technology* 49, 39-53.

Gauer, P., Kern, M., Kristensen, K., Lied, E., Rammer, L., Schreiber, H. 2007. On pulsed Doppler radar measurements of avalanches and their implication to avalanche dynamics, *Cold Regions Science and Technology* 50, 55-71.

Iverson, R. M. 2013. Debris flows: behaviour and hazard assessment, *Geology Today*

Kern, M.A., Bartelt, P.A., Sovilla, B. 2010. Velocity profile inversion in dense avalanche flow, *Annals of Glaciology* 51, 27-31.

Rammer, L., Kern, M., Gruber, U., and Tiefenbacher, F. 2007. Comparison of avalanche-velocity measurements by means of pulsed Doppler radar, continuous wave radar and optical methods. *Cold Regions Science and Technology* 50, 35-54.

Sovilla, B., Burlando, P., Bartelt, P. 2006. Field experiments and numerical modelling of mass entrainment in snow avalanches, *Journal of Geophysical Research* 111, F03007, doi:10.1029/2005JF000391.

Sovilla, B., Schaer, M., Kern, M., Bartelt, P. 2008. Impact pressures and flow regimes in dense snow avalanches observed at the Vallée de la Sionne test site, *Journal of Geophysical Research* 113, F01010, doi:10.1029/2006JF000688.

Vriend, N.M., McElwaine, J.N., Sovilla, B., Keylock, C.J., Ash, M., Brennan, P.V. 2013. High resolution radar measurements of snow avalanches, *Geophysical Research Letters* 40, 5, doi:10.1002/grl.50134.

Figure 1. A large-scale avalanche at the Vallée de la Sionne test site just about to reach the instrument pylon.

Figure 2. Avalanche damage after the fatal October 1995 avalanche in Flateyri, Iceland. Image courtesy of the Icelandic Meteorological Office.
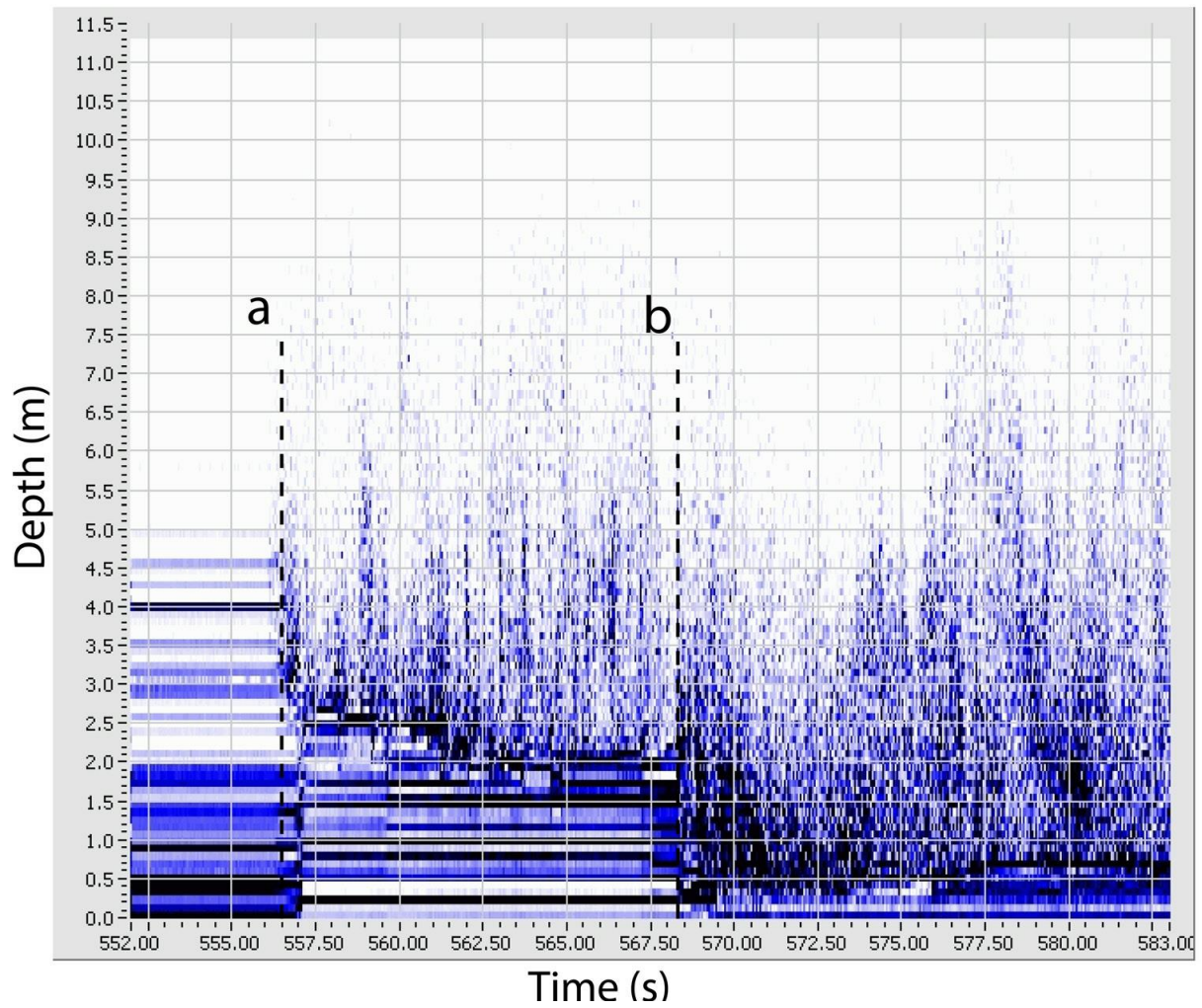
Figure 3. Entrainment of snow by an avalanche monitored by an upward looking radar
system. The front of the avalanche arrives at (a) and there is steady entrainment
between (a) and (b). At (b) there is a sudden entrainment of 1.5 m of snow as the dense
part of the avalanche passes over the radar. This figure is reproduced from Sovilla, B.,
Burlando, P. and Bartelt, P. 2006. Field experiments and numerical modelling of mass
entrainment in snow avalanches, *Journal of Geophysical Research* 111, F03007,
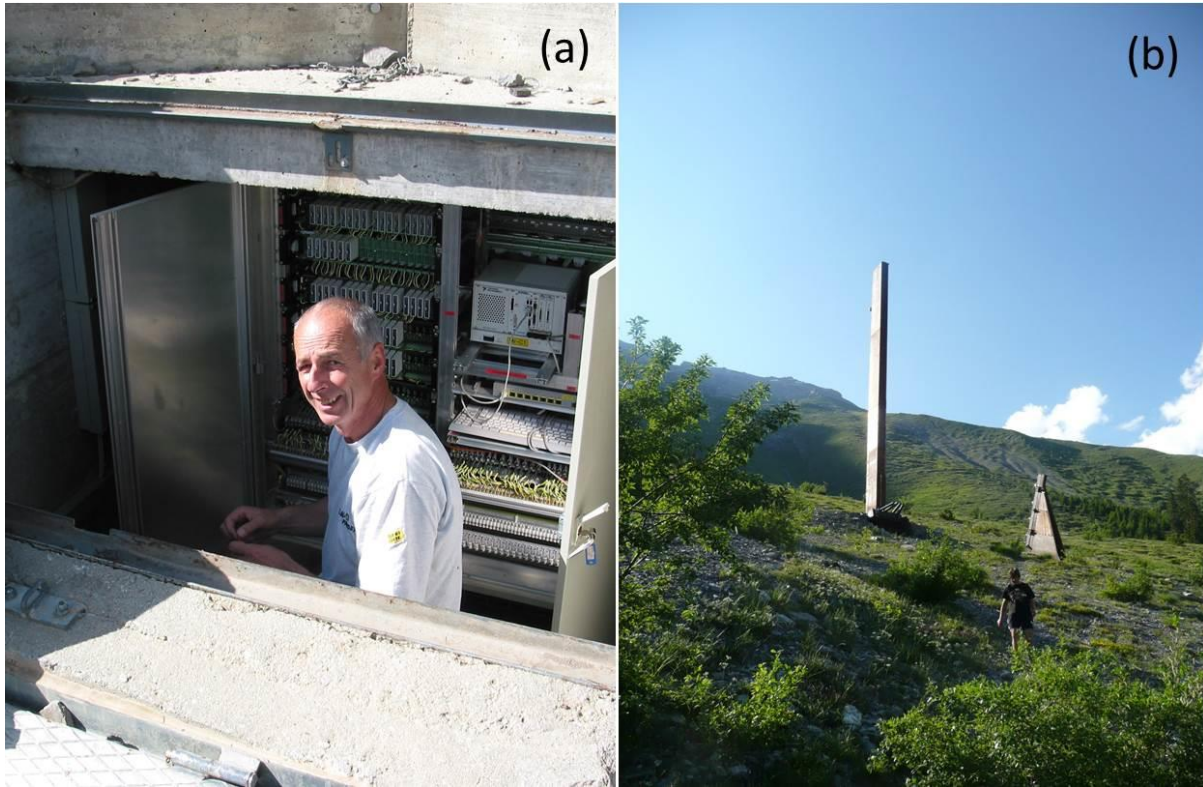doi:10.1029/2005JF000391 with the permission of the American Geophysical Union.

Figure 4. Martin Hiller of SLF checking the electronics for the sensors in the avalanche path (a). In (b) are shown the main instrument pylon (also seen in Fig. 1) and the wedge containing the load cells.
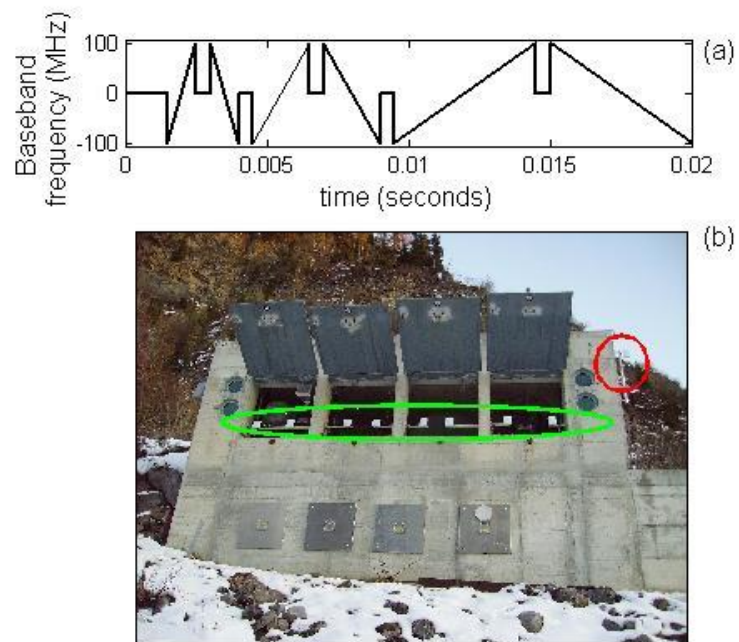
Figure 5. Our set of transmitted up and down chirps is shown in (a), while (b) shows the avalanche bunker at Vallée de la Sionne with the shutters open and our transmitter mounted on the side of the bunker (red circle) and one set of eight receivers (green ellipse).
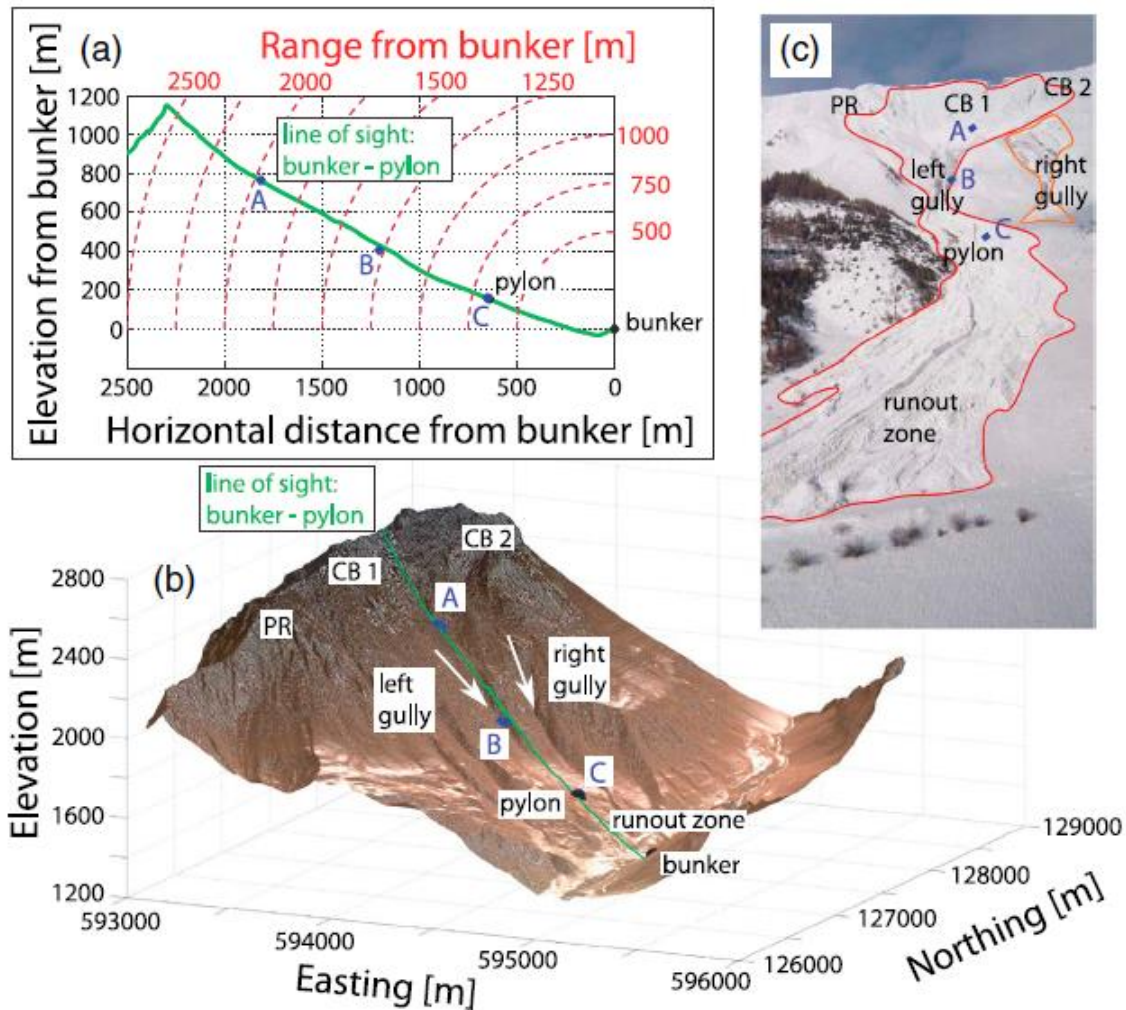
Figure 6. A cross-section of the avalanche path at Vallée del a Sionne (a), together with a three-dimensional rendering of the topography (b) and an image of the path from the bunker (c). *PR*, *CB1* and *CB2* are abbreviations for particular release regions while the blue letters *A*, *B* and *C* show the approximate locations of the buried, upward looking radar pairs discussed in the text. The figure is reproduced from: Vriend, N.M., McElwaine, J.N., Sovilla, B., Keylock, C.J., Ash, M., Brennan, P.V. 2013. High resolution radar measurements of snow avalanches, *Geophysical Research Letters* 40, 5, doi:10.1002/grl.50134 with the permission of the American Geophysical Union.
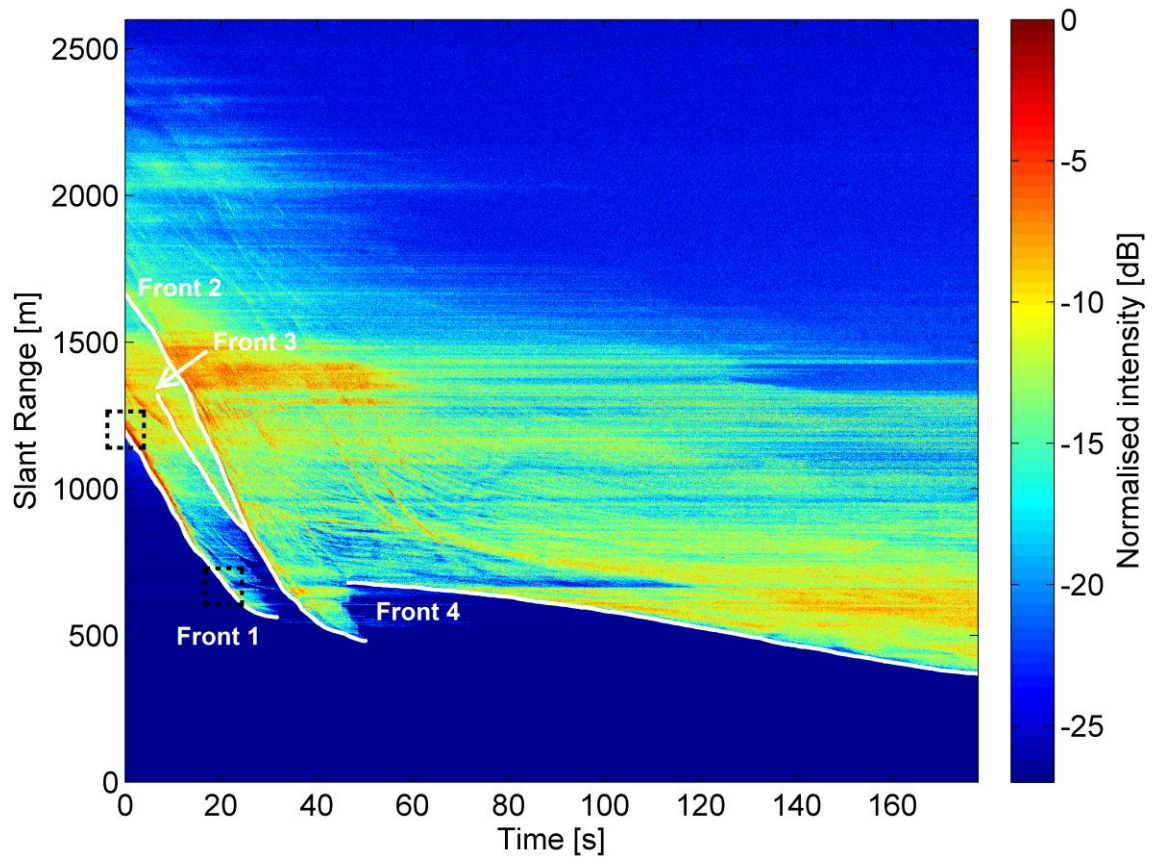
THIS ONE WITH THE SQUARE BOXES AND FRONTS REMOVED, EXCEPT FOR FRONT 1 AND WHAT I THINK IS FRONT 1B (UNMARKED BETWEEN FRONT 1 AND FRONT 3) AS WELL AS A HIGHLIGHTING OF THE FRONTS BEHIND THE MAIN FRONT (MENTIONED IN THE DISCUSSION, HENCE DIFFERENT TO THE FIGURE MATT SUBMITTED)?

Figure 7. A range versus time plot of an example recorded avalanche. This is a moving time indication (MTI) image, where dark red indicates a very strong return.